The effect of high driving force on the methane hydrate-polyvinylpyrrolidone system

*Dany Posteraro, Jonathan Verrett, Milan Maric, Phillip Servio**

Department of Chemical Engineering, McGill University, Montreal, Quebec, Canada

Polymer based kinetic hydrate inhibitors are increasingly used in the oil and gas industry to prevent hydrate formation. It is well known that the effectiveness of inhibitors decreases as the driving force for hydrate formation increases. The current study assesses whether the inhibitory effect of polyvinylpyrrolidone (PVP) can be completely masked by high driving forces for hydrate growth. Methane hydrate kinetic experiments were performed with solutions of pure water and 0.007 wt% PVP in water at 277 K and pressures ranging from 23.83 MPa to 31.33 MPa. Results showed that as the driving force for hydrate formation increases, the effect of PVP as a hydrate growth inhibitor diminishes and may be entirely masked for a significant amount of time. With the current system, hydrate growth appeared uninhibited at subcoolings greater than 17.4 K (26.33 MPa). The time of uninhibited growth was found to increase linearly with subcooling to a maximum of 537 s at a 19K subcooling (31.33 MPa). Under such high driving forces, inhibitory effects have been shown to take time to manifest themselves, indicating that under these conditions additives have no effect on hydrate nucleation but solely on hydrate growth following nucleation.

***Corresponding Author. Telephone:** *+1-514-398-1026.* **Fax:** *+1-514-398-6678.* **E-mail:** *phillip.servio@mcgill.ca*

Key Words:

Clathrate hydrate
Methane
Growth
High driving force
Inhibition
Polyvinylpyrrolidone (PVP)

Abbreviations:

AA	Anti-agglomerant
KHI	Kinetic hydrate Inhibitor
LDHI	Low-dosage hydrate Inhibitor
PVP	Polyvinylpyrrolidone
PVCap	Polyvinylcaprolactam
RO	Reverse osmosis
THI	Thermodynamic hydrate inhibitor
SDS	Sodium dodecyl sulfate
SARA	Saturate Aromatic Resin Asphaltene

Notation:

$AARE$	Average absolute relative error (%)
$_{avg}$	Average
$_{exp}$	Experimental
i	Number of experimental replicates spanning from 1 to r_t
k	Timestep following nucleation, in seconds, spanning from 1 to t_t
ΔT	Subcooling (K)
y	Cumulative gas consumption (moles)

I. INTRODUCTION

Clathrate hydrates are non-stoichiometric crystalline compounds formed from a guest molecule interacting with a liquid water cage under suitable thermodynamic conditions (Sloan and Koh, 2008). Notably described by Sir Humphry Davy in 1811 (Davy, 1811), it was not until the 1930's that gas hydrates were linked to industry, undoubtedly increasing the demand for hydrate research (Hammerschmidt, 1934). Recently, methane hydrates have been intensely investigated for their potential as a vast future energy source, and risk to global climate (Englezos, 1993; Kvenvolden, 1999). It has been estimated that approximately 53% of all carbon-based resources available on earth are stored in hydrate form (Kvenvolden, 1988; Lee and Holder, 2001).

Hydrate inhibitors have long been a subject of interest to the oil and gas industry due to their potential use for flow assurance in oil and gas pipelines (Kelland, 2006; Sloan et al., 2010). If operating under suitable thermodynamic conditions, gas hydrates have been known to cause blockages to oil pipelines and further complications to drilling operations, as exemplified by the oil spill in the Gulf of Mexico in 2010 (Jernelöv, 2010). A common prevention method is to use additives such as methanol to shift the phase boundary for hydrate formation (Anderson and Prausnitz, 1986). Such additives are called thermodynamic hydrate inhibitors (THIs) (Sloan, 2003). They have been found to be effective but often require large quantities of the inhibitor (Frostman et al., 2003). Low-dosage hydrate inhibitors (LHDIs) attempt to respond to this problem and are commonly categorized as anti-agglomerants (AAs) or kinetic hydrate inhibitors (KHIs) (Igboanusi and Opara, 2011). AAs act by preventing aggregation of small hydrate crystals into a large blockage whereas KHIs aim to prevent nucleation or growth (Gao, 2009).

Presently, the most commonly researched KHIs are polyvinylpyrrolidone (PVP) and polyvinylcaprolactam (PVCap) (Anderson et al., 2005; Kelland, 2006). Both these compounds

have been found to affect nucleation and hydrate growth due to their lactam ring structures (Perrin et al., 2013). The mechanism is still not fully understood but a variety of possibilities have been proposed in the literature. During nucleation, the lactam ring is thought to prevent the formation of stable nuclei by affecting the arrangement of water cages or disrupting nuclei before they reach a critical size (Yang and Tohidi, 2011). Following nucleation, lactam structures are believed to inhibit growth by adsorbing to the crystal surface, thus limiting the area available for hydrate growth (Carver et al., 1995; Ivall et al., 2015; Kvamme et al., 1997; O'Reilly et al., 2011).

Initially and even today, many studies focus on testing KHIs as nucleation inhibitors (Daraboina and Linga, 2013; Lone and Kelland, 2013). Emphasis has shifted to testing KHIs as growth inhibitors following nucleation, although there is still a notable lack of data in this area (Anderson et al., 2011). It has been previously shown that at a given constant KHI concentration, hydrate inhibition decreases as driving force increases (Al-Adel et al., 2008). This work aims to further characterize the relationship between the driving force for hydrate formation and the inhibitory effects of KHIs and determine whether such effects can be completely masked.

II. EXPERIMENTAL METHODS

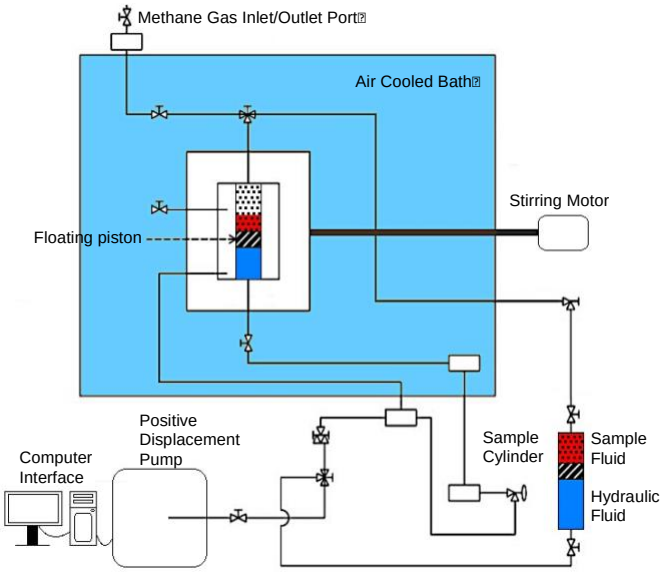

Figure 1. Schematic diagram of the Jefri Direct Behaviour Rating system.

A. APPARATUS - The Jefri Direct Behavior Rating system shown in Figure 1 was used to assess the effect of high driving forces on methane hydrate-PVP systems (Schlumberger Model Number: PVT-150-10-155 [Pressure-Volume-Temperature]). This set-up consists of a crystallizer capable of operating at a maximum pressure of 31.33 MPa. The crystallizer is made of a 20-cm-long fused quartz cylinder with a total internal volume of 150 cm^3. The cylinder contains the test solution and is enclosed in a stainless steel frame. To view the test solution during experimentation, the frame has two glass side windows. The system maintains a constant operating pressure using a floating piston to account for volume changes. The pressure is manipulated using a positive displacement pump connected to the piston via a hydraulic fluid channel. The cell as a whole is mounted to a steel bracket and attached to a motor, allowing it to oscillate at a 120-degree angle at a speed of 40 cycles per minute to mix the sample. The entire system is contained in an air-cooled chamber allowing temperature control. A platinum

resistance temperature detector (RTD) probe and a pressure transducer are used to measure crystallizer temperature and pressure, respectively. The system comes equipped with its own temperature display unit and interface pump program and monitors the temperature, pressure and volume displaced in the crystallizer. The standard uncertainty for temperature and pressure measurements were estimated to be U_T = 0.1 K and U_p = 14 kPa, respectively.

B. MATERIALS – Polyvinylpyrrolidone (PVP) was obtained from Sigma Aldrich in powder form with an average molecular weight of 10,000 g/mol. The methane gas used was ultra-high purity in excess of 99.99% obtained from MEGS Inc. Reverse Osmosis (RO) water is produced on-site using four polyamide-composite thin-film membranes in a system supplied by Dow Filmtec. The water has a final conductivity of 10 μS/cm and total organic content less than 10 ppb with salt rejection larger than 99%.

C. PROCEDURE - To begin the high pressure kinetic experiments, the entire system is cooled to the experimental temperature of 277 K. Prior to sample injection, the crystallizer is rinsed with 140 mL of RO water five times to remove any potential contaminants. A testing sample of 16.5 mL of either RO water or PVP solution is then injected into the reactor. The pressure within the reactor is then increased to 2 MPa and subsequently depressurized to 150 kPa four times to ensure that methane is the only potential hydrate former present. A reading above atmospheric pressure (150 kPa) is chosen in order to prevent air flow back into the system. Once thermal equilibrium has been attained, the pressure is increased to the desired experimental value using the positive displacement pump. Recording of the temperature, pressure and volume commences and the mixer is activated. Since the pressure (i.e. driving force) is extremely high, the formation of hydrates is relatively quick (< 1 minute). A visual inspection is therefore performed to verify the point of turbidity (hydrate formation). Due to the exothermic nature of hydrate

crystallization, a temperature change in solution is also observed further validating turbidity and the time is noted. Following formation, the hydrates are left to grow for 1300 s.

Once the experiment is complete, the recorder and mechanical mixer are stopped. The crystallizer is depressurized to 100 kPa to decompose and remove all gas hydrates and methane from the reactor. Another sample then is injected using the aforementioned procedure. At this point, the temperature, pressure and volume displacement data are exported and analyzed using the Trebble-Bishnoi equation of state, which converts the volume displaced to moles of methane consumed (Trebble and Bishnoi, 1987).

III. RESULTS AND DISCUSSION

Table 1. Summary of experimental conditions, induction times, growth characteristics and variation between runs. Induction time values include 95% confidence intervals.

absolute pressure (MPa)	subcooling (K)	PVP concentration (wt%)	Induction time (s)	uninhibited growth time (s)	AARE (%)
23.83	16.5	0	5 ± 3	-	6.87
23.83	16.5	0.007	18 ± 13	0	4.78
26.33	17.4	0.007	9 ± 5	0	7.87
26.70	17.5	0.007	12 ± 5	23	4.43
27.08	17.7	0.007	8 ± 5	95	3.34
27.83	17.9	0.007	7 ± 3	173	7.50
28.83	18.2	0	6 ± 2	-	2.39
28.83	18.2	0.007	6 ± 7	253	1.09
31.33	19	0	5 ± 9	-	4.25
31.33	19	0.007	11 ± 14	537	3.49

The purpose of these high-pressure tests was to determine if a substantial driving force could completely mask the effect of PVP on hydrate growth kinetics. High-pressure kinetic experiments were first conducted with RO water and then compared to a solution of 0.007 wt% PVP in RO water. This concentration of PVP was chosen to coincide with previous publications, which determined this concentration to be sufficient for hydrate growth inhibition (Al-Adel et al., 2008; Posteraro et al., 2015). A similar approach was used to determine the testing concentration of sodium dodecyl sulfate (SDS) to determine its effect on dissolution (Posteraro et al., 2016). Solutions of PVP were all tested at 277 K and a variety of pressures as shown in

Table 1. In order to define a driving force for the given system, two different methodologies may be applied. The first method is defined in terms of pressure (ΔP) while the second is defined in terms of temperature, commonly known as subcooling (ΔT). The driving force for hydrate growth in the present system is expressed in terms of subcooling, which is the difference between the experimental temperature and the equilibrium temperature at the experimental pressure. Equilibrium temperatures were obtained from a previous study conducted by Frost and Deaton (Frost and Deaton, 1946). Subcooling is commonly used to represent crystallization driving force in hydrate systems (Kelland, 2006). It has been found that for systems with a single gas species, such as the current one with methane, there is no significant difference in expressing a driving force in terms of pressure or subcooling (Arjmandi et al., 2005). Gas consumption data obtained at a sample test condition, in this case 0.007 wt% PVP at 17.5 K subcooling, can be seen for each replicate in Figure 2. Each experimental condition was tested seven times with fresh samples (previously unused samples) so as to assess reproducibility. The peaks in data represent the injection of gas into the system to keep system pressure constant. The final gas consumption curves presented in Figure 3 were the averages of the individual gas consumption data collected at each condition. Differences between replicates were characterized using the absolute average relative error (AARE) formula given by Equation (1), where y is the cumulative gas consumption, k denotes the timestep following nucleation (in seconds) spanning from 1 to t_t, i is the number of replicates spanning from 1 to r_t, and the experimental and average values are denoted by the exp and avg superscripts, respectively. The AARE for all samples tested can be found in Table 1. All AARE values are well below 10%, which is consistent with previous studies with similar systems given the variety of hydrodynamic conditions that may be encountered (Posteraro et al., 2015; Verrett and Servio, 2012).

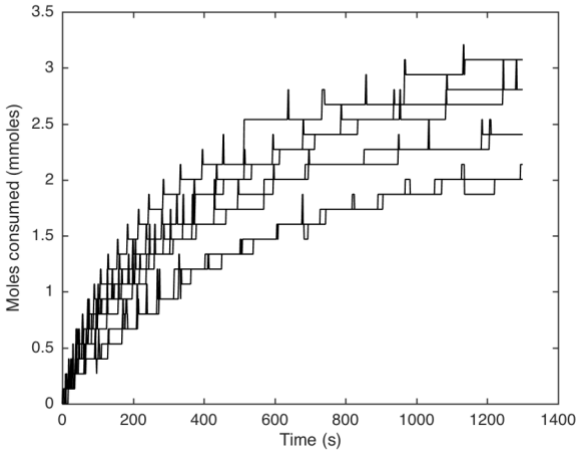

Figure 2. Replicates of cumulative mole consumption over time following hydrate formation at 0.007 wt% PVP solution and 17.5 K subcooling.

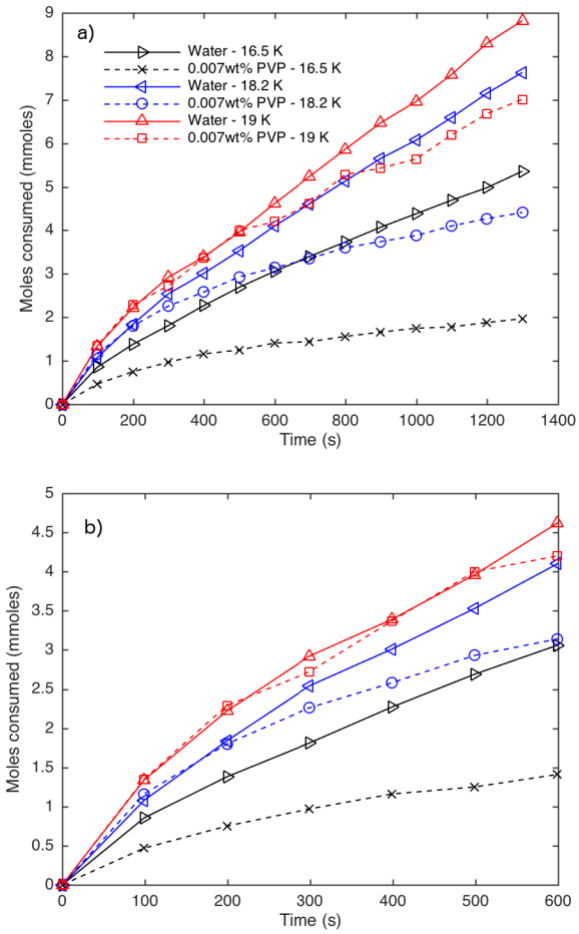

Figure 3. Cumulative mole consumption over time following hydrate formation for RO water (solid lines) and 0.007 wt% PVP solution (dashed lines) at 16.5 K subcooling (black), 18.2 K subcooling (blue) and 19 K subcooling (red). Image a) shows growth over the entire period measured from 0 to 1300 s, image b) is a magnification of the first 600 s.

$$\%\ AARE = \frac{100}{t_t * r_t} \sum_{k=1}^{t_t} \sum_{i=1}^{r_t} \frac{\left| y_{k,i}^{exp} - y_k^{avg} \right|}{y_k^{avg}} \quad \text{(Equation 1)}$$

To establish baselines, RO water solutions were tested at 16.5, 18.2 and 19 K subcoolings. The average gas consumption over time following nucleation for each of these samples can be seen in Figure 3. PVP samples at a concentration of 0.007 wt% were also tested at these same conditions with the resulting gas consumption curves shown in Figure 3. The water and PVP curves at a 16.5 K subcooling show a distinct separation immediately following nucleation, indicating that PVP is affecting hydrate growth from the onset of nucleation. This is consistent with previous experiments and may be due to PVP effects at the nucleation or growth stages (Glénat et al., 2011; Posteraro et al., 2015). Curves at higher subcoolings are initially similar and then deviate after a point in time. This indicates that PVP is not having an effect at the nucleation stage because gas consumption for both solutions is initially similar. To further validate this observation, the reported induction times are extremely short and show no significant differences between the induction times for water and the PVP samples. At some point during the growth stage, PVP begins to affect hydrate growth and gas consumption slows. This deviation was characterized using Equation (2) to calculate the relative deviation between the RO water and PVP curves for every point in time. PVP was deemed to inhibit growth if the relative deviation was greater than 0.05, meaning that the difference between the gas consumed by the RO water

and PVP samples was greater than 5%. The amount of time following nucleation with uninhibited growth, meaning a deviation less than 5%, can be seen in Table 1.

$$relative\ deviation_k = \frac{|y_k^{RO} - y_k^{PVP}|}{y_k^{RO}} \text{ (Equation 2)}$$

To further characterize the relationship between uninhibited growth time and subcooling, additional experiments were performed at subcoolings between 16.5 K and 18.2 K. RO water tests were not performed at these conditions. PVP data was instead compared to weighted averages using the 16.5 K and 19 K RO water runs. To validate this assumption, these RO water runs were used to estimate gas consumption at an 18.2 K subcooling and compared to the measured PVP data. The time range of interest for this data is up to 253 s, since uninhibited growth times for subcoolings lower than 18.2 K should be less than the uninhibited growth time at 18.2 K subcooling. The AARE between the weighted average and the measured data up to 253 s was 1.85%, which is small compared to the error between runs, and demonstrates these weighted baselines can be used for comparison in this timeframe. The uninhibited growth time was calculated for these additional PVP samples using these weighted baselines and can be found in Table 1. Note that all the uninhibited growth times were found to be below 253 s, consistent with the assumption made previously about the time range for uninhibited growth. These times increase with increasing subcooling, showing PVP is less effective at inhibiting hydrate growth as driving force increases. Uninhibited growth time is plotted against subcooling in Figure 4. Initially there is no uninhibited growth time, but above 17.4 K subcooling, a linear trend can be seen. The linear relationship between subcooling above 17.4 K and uninhibited growth time for this system is expressed in Equation (3).

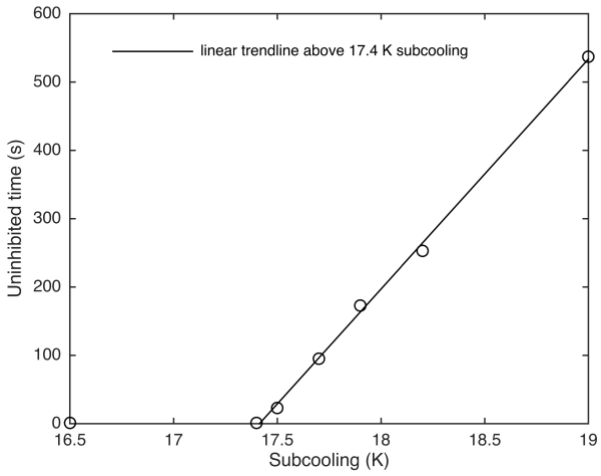

Figure 4. Amount of time during which hydrate growth is uninhibited at various subcoolings. A linear trendline is included for uninhibited samples above 17.4 K subcooling.

$$unihibted\ growth\ time\ (s) = 336\frac{s}{K} * \Delta T(K) - 5860s \quad \text{(Equation 3)}$$

Note that the relationship between uninhibited time and subcooling or driving force is linear. Future studies could be undertaken to determine whether a linear relationship is characteristic for all kinetic hydrate inhibitors and may provide insight on the inhibition mechanism or help classify inhibitors. In the case of this experiment, we postulate that the equation constants (slope and intercept) would change based on the PVP concentration as well as the system's temperature and hydrodynamic conditions. The result is significant as it indicates that PVP's effects, and possibly the effects of other inhibitors, can be completely masked above a certain driving force for a significant amount of time under hydrate forming conditions. These results demonstrate the need to assess the effectiveness of kinetic growth inhibitors at high driving forces prior to implementation, as their effects may be negligible. Furthermore, for purposes involving pipeline applications, additional testing may be required depending on the operating pressures used.

Previous studies on nucleation and growth have also been performed on various systems including high pressure semi-batch crystallizers, high-pressure micro-differential scanning calorimeters and high pressure rocking cells. Although no other studies to date have shown initial uninhibited hydrate growth with KHI's, some studies have shown a decrease in nucleation efficiency (reduction of nucleation inhibitor strength). In a study conducted by Daraboina et al. (2015), a rocking cell was used in order to determine natural gas hydrate formation and inhibition effects using a gas/crude oil/aqueous system (Daraboina et al., 2015). Luvicap-Bio, a biodegradable commercial kinetic hydrate inhibitor, was used in a set of experiments containing 30% crude oil (fractional composition of crude by SARA analysis (0.8515 g/cc) was paraffins 51; aromatics 9; resins 4 and asphaltenes 36) (Pachitsas, 2014) and natural gas as the hydrate former. The results of these tests indicated that the nucleation inhibition strength of Luvicap-Bio decreased in the presence of crude oil compared to the same non-crude containing sample (Daraboina et al., 2015). In another study conducted by Sharifi et al. (2013), a similar result was also attained upon the addition of n-heptane (liquid hydrocarbon) to solutions of PVP and PVCap (Sharifi et al., 2013). It is important to note that in both of these systems including the present study, the efficiency of the inhibitor used was reduced in one way or another. Due to the latter observations, it may be possible to correlate the addition of specific crude oils to a system (decrease water cut) to the effect of using a higher driving force on a simplified system. If the above correlation is determined, it may be possible to establish a link between a simplified system and an actual scenario in need of investigation. However, much work using a variety of systems would need to be done to obtain this objective.

Inhibitors such as PVP are generally thought to function by disrupting hydrate nucleation or adsorbing to the hydrate surface during growth (Anderson et al., 2005; Carver et al., 1995;

Kvamme et al., 1997; Perrin et al., 2013). The high driving forces used in this study appear to prevent the inhibitor from affecting nucleation (Al-Adel et al., 2008). A possible explanation for this phenomenon may be a large number of hydrate nuclei created at high driving forces (Servio and Englezos, 2003; Sloan and Koh, 2008). This large number of nuclei may create too large of a surface area for PVP to impact (Yang and Tohidi, 2011). As growth continues, hydrates may agglomerate and thus reduce their overall surface area, allowing PVP to inhibit growth. Further studies analyzing particle size distribution during growth under such conditions would be useful, but may be challenging given the extreme conditions.

IV. CONCLUSIONS

High-pressure methane hydrate kinetic experiments were performed with solutions of reverse osmosis water and 0.007 wt% PVP at 277 K and pressures ranging from 23.83 MPa to 31.33 MPa. Results showed that as the driving force for hydrate formation increases, the effect of PVP as a hydrate inhibitor diminishes and may be entirely masked for a significant amount of time. With the current system, hydrate growth appeared uninhibited at subcoolings greater than 17.4 K and the time of uninhibited growth increased linearly with subcooling to a maximum of 537 s. At such high driving forces PVP appears to have no effect during hydrate nucleation, but eventually appears to have an effect on growth.

ACKNOWLEDGMENTS

The authors are grateful to the Natural Sciences and Engineering Research Council of Canada (NSERC), les Fonds de Recherche du Québec - Nature et Technologies (FRQNT), the Canada Research Chair program (CRC), Imperial Oil, the McGill University Faculty of Engineering

(MEDA scholarship) and the McGill University Department of Chemical Engineering (EUL scholarship) for financial support.

REFERENCES

Al-Adel, S., Dick, J. A. G., El-Ghafari, R., Servio, P., 2008. The effect of biological and polymeric inhibitors on methane gas hydrate growth kinetics. Fluid Phase Equilibr. 267, (1), 92-98.

Anderson, B. J., Tester, J. W., Borghi, G. P., Trout, B. L., 2005. Properties of Inhibitors of Methane Hydrate Formation via Molecular Dynamics Simulations. J. Am. Chem. Soc. 127, (50), 17852-17862.

Anderson, F., Prausnitz, J., 1986. Inhibition of gas hydrates by methanol. AIChE J. 32, (8), 1321-1333.

Anderson, R., Mozaffar, H., Tohidi, B. 2011. Development of a crystal growth inhibition based method for the evaluation of kinetic hydrate inhibitors. Proceedings of the 7th International Conference on Gas Hydrates.

Arjmandi, M., Tohidi, B., Danesh, A., Todd, A. C., 2005. Is subcooling the right driving force for testing low-dosage hydrate inhibitors? Chem. Eng. Sci. 60, (5), 1313-1321.

Carver, T. J., Drew, M. G. B., Rodger, P. M., 1995. Inhibition of crystal growth in methane hydrate. J. Chem. Soc. Faraday T. 91, (19), 3449-3460.

Daraboina, N., Linga, P., 2013. Experimental investigation of the effect of poly-N-vinyl pyrrolidone (PVP) on methane/propane clathrates using a new contact mode. Chem. Eng. Sci. 93, 387-394.

Daraboina, N., Pachitsas, S., von Solms, N., 2015. Natural gas hydrate formation and inhibition in gas/crude oil/aqueous systems. Fuel. 148, (2015), 186-190.

Davy, H., 1811. On a combination of Oxymuriatic Gas and Oxygene Gas. Philos. T. R. Soc. Lond. 101, 155-162.

Englezos, P., 1993. Clathrate hydrates. Ind. Eng. Chem. Res. 32, (7), 1251-1274.

Frost, E. M., Jr., Deaton, W. M., 1946. Gas hydrate composition and equilibrium data. Oil Gas J. 45, 170-8.

Frostman, L., Thieu, V., Crosby, D., Downs, H. 2003. Low-Dosage Hydrate Inhibitors (LDHIs): Reducing Costs in Existing Systems and Designing for the Future. International Symposium on Oilfield Chemistry, SPE.

Gao, S., 2009. Hydrate risk management at high watercuts with anti-agglomerant hydrate inhibitors. Energ. Fuel. 23, (4), 2118-2121.

Glénat, P., Anderson, R., Mozaffar, H., Tohidi, B. 2011. Application of a new crystal growth inhibition based KHI evaluation method to commercial formulation assessment. Proceedings of the 7th International Conference on Gas hydrates.

Hammerschmidt, E., 1934. Formation of gas hydrates in natural gas transmission lines. Ind. Eng. Chem. 26, (8), 851-855.

Igboanusi, U., Opara, A. C., 2011. The Advancement from Thermodynamic Inhibitors to Kinetic Inhibitors and Anti-Agglomerants in Natural Gas Flow Assurance. Int. J. Chem. Environ. Eng. 2, (2), 131-134.

Ivall, J., Pasieka, J., Posteraro, D., Servio, P., 2015. Profiling the Concentration of the Kinetic Inhibitor Polyvinylpyrrolidone throughout the Methane Hydrate Formation Process. Energ. Fuel. 29, (4), 2329-2335.

Jernelöv, A., 2010. The threats from oil spills: Now, then, and in the future. Ambio. 39, (5-6), 353-366.

Kelland, M. A., 2006. History of the development of low dosage hydrate inhibitors. Energ. Fuel. 20, (3), 825-847.

Kvamme, B. B., Huseby, G., Forrisdahl, O. K., 1997. Molecular dynamics simulations of PVP kinetic inhibitor in liquid water and hydrate/liquid water systems. Mol. Phys. 90, (6), 979-992.

Kvenvolden, K. A., 1988. Methane hydrate. A major reservoir of carbon in the shallow geosphere? Chem. Geol. 71, (1-3), 41-51.

Kvenvolden, K. A., 1999. Potential effects of gas hydrate on human welfare. P. Natl. Acad. Sci. U. S. A. 96, (7), 3420-3426.

Lee, S.-Y., Holder, G. D., 2001. Methane hydrates potential as a future energy source. Fuel Process. Technol. 71, (1), 181-186.

Lone, A., Kelland, M. A., 2013. Exploring Kinetic Hydrate Inhibitor Test Methods and Conditions Using a Multicell Steel Rocker Rig. Energ. Fuel. 27, (5), 2536-2547.

O'Reilly, R., Ieong, N. S., Chua, P. C., Kelland, M. A., 2011. Crystal growth inhibition of tetrahydrofuran hydrate with poly(N-vinyl piperidone) and other poly(N-vinyl lactam) homopolymers. Chem. Eng. Sci. 66, (24), 6555-6560.

Pachitsas S, 2014. The effect of oils on hydrate formation in natural gas pipelines, Masters Thesis: Chemical and Biochemical Engineering, Technical University of Denmark.

Perrin, A., Musa, O. M., Steed, J. W., 2013. The chemistry of low dosage clathrate hydrate inhibitors. Chem. Soc. Rev. 42, 1996-2015.

Posteraro, D., Pasieka, J., Maric, M., Servio, P., 2016. The Effect of Hydrate Promoter SDS on Methane Dissolution Rates at the Three Phase (H-Lw-V) Equilibrium Condition. J. Nat. Gas Sci. Eng. In Press, Accepted Manuscript.

Posteraro, D., Verrett, J., Maric, M., Servio, P., 2015. New insights into the effect of polyvinylpyrrolidone (PVP) concentration on methane hydrate growth. 1. Growth rate. Chem. Eng. Sci. 126, 99-105.

Servio, P., Englezos, P., 2003. Morphology of Methane and Carbon Dioxide Hydrates Formed from Water Droplets. A. I. Ch. E. J., 49(1), 269-276.

Sharifi, H., Ripmeester, J., Walker, V. K., Englezos. P., 2014. Kinetic inhibition of natural gas hydrates in saline solutions and heptane. Fuel. 117, (2014), 109-117.

Sloan, E. D., 2003. Fundamental principles and applications of natural gas hydrates. Nature. 426, 353-363.

Sloan, E. D., Koh, C. A., 2008. Clathrate Hydrates of Natural Gases. CRC Press: Boca Raton, FL. (Chapter 1 pp. 6-9; Chapter 2 pp. 45-102; Chapter 3 pp. 158)

Sloan, E. D., Koh, C. A., Sum, A., 2010. Natural gas hydrates in flow assurance. Gulf Professional Publishing. (Chapter 5 pp. 87-103; Chapter 6 pp. 105-135; Chapter 7 pp. 152)

Trebble, M. A., Bishnoi, P. R., 1987. Development of a new four-parameter cubic equation of state. Fluid Phase Equilibr. 35, (1-3), 1-18.

Verrett, J., Servio, P., 2012. Evaluating surfactants and their effect on methane mole fraction during hydrate growth. Ind. Eng. Chem. Res. 51, (40), 13144-13149.

Yang, J., Tohidi, B., 2011. Characterization of inhibition mechanisms of kinetic hydrate inhibitors using ultrasonic test technique. Chem. Eng. Sci. 66, (3), 278-283.